CRYSTAL GROWTH & DESIGN

Article

pubs.acs.org/crystal

Probability of Nucleation in a Metastable Zone: Induction Supersaturation and Implications

Venkateswarlu Bhamidi,*,† Paul J. A. Kenis, and Charles F. Zukoski

Department of Chemical & Biomolecular Engineering, University of Illinois at Urbana−Champaign, 600 South Mathews Avenue, Urbana, Illinois 61801, United States

Supporting Information

ABSTRACT: The metastable zone in solution crystallization is typically defined as a region of the phase diagram in which no appreciable nucleation occurs. Existing theoretical explanations attribute the appearance of this zone to the low probability of nucleation brought forth by the path-dependency of the nucleation rate. In this work, for the first time we present experimental data for several compounds that contradict this description. We show that the widely adopted theoretical approach which considers a time-dependent nucleation rate does not capture the observed stochastic nature of nucleation in these experiments. Instead, the experimental results are successfully explained through a probability analysis based solely on the energy barrier to nucleation. In this context, for a system that is slowly supersaturated, we develop the idea of an "induction supersaturation" as a lower boundary of metastability that does not depend on the path of the experiment. This work critically examines the limitations of the existing stochastic methods that describe nucleation under variable supersaturation and calls for a fundamental shift in the traditional view of the processes responsible for the manifestation of the metastable zone.

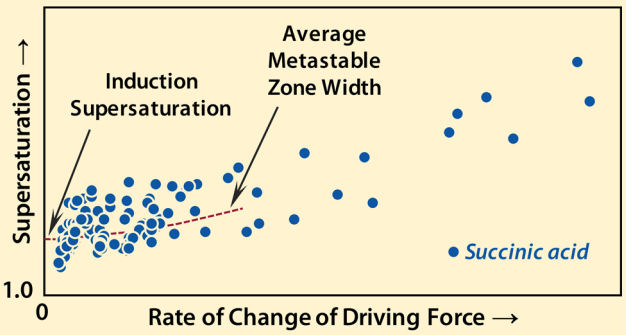

1. INTRODUCTION

Formation of crystals from solutions is of great importance in several areas of science and technology.[1−6] The metastable zone in solution crystallization is defined as a region of the phase diagram characterized by the absence of appreciable nucleation.[7] Characterization of the width of this metastable region (also known as the metastable zone width, MZW) for a compound is considered to provide an important guideline for the design and operation of industrial crystallizers.[8] Thus, the prediction of the probability of nucleation at any solution condition when a system is gradually driven toward phase transformation is of significant interest.

The driving force for crystal nucleation is the change in the chemical potential of the solute, $\Delta\mu$, resulting from the phase transformation. This chemical potential difference $\Delta\mu$ is expressed through the supersaturation, S, of the solute, which is defined here as the ratio of solute concentration C to its solubility C_{eq} ($S = C/C_{eq}$).[9] Experimentally, the MZW of a compound may be determined by gradually increasing the supersaturation of the system starting from an $S \leq 1$ to a supersaturation S_n at which the first crystals are observed. This S_n may be obtained either by lowering the temperature of a solution (cooling crystallization at a constant composition) or by increasing the concentration the solute (evaporative crystallization at a constant temperature).[7]

The most common experimental technique employed to determine the MZW of a solute is cooling crystallization with constant rate of cooling. Studies that use this technique consistently show that greater rates of cooling result in larger values of undercooling (i.e., wider metastable zone width).[10,11] These observations give rise to the notion that the MZW is a kinetic phenomenon that is controlled by the path of the experiment. As a result, over the past several decades, theoretical approaches developed to predict the boundary of metastability have focused on linking the path of the experiment (rate of cooling) to the rate of the nucleation.[12−17] These models typically consider the MZW as a deterministic phenomenon. Nucleation, however, is inherently a stochastic process, and hence one expects a variability in an experimentally determined limit of metastability. Analysis of such variability in the time of nucleation for systems nucleating *isothermally* (i.e., at constant temperature or supersaturation) was discussed by Sear.[18]

Recently, in an experimental study that used evaporative crystallization at constant temperature, He et al. (from our group) have reported a seemingly path-independent critical supersaturation (MZW) observed for several solutes.[19] Intrigued by this unexpected result that contradicts the typical observations from cooling crystallization, Braatz and co-workers, along with us, have developed a rigorous stochastic model to estimate the "mean time" of nucleation t_n in these experiments.[20] This work

Received: October 18, 2016
Revised: December 26, 2016
Published: January 27, 2017

DOI: 10.1021/acs.cgd.6b01529
Cryst. Growth Des. 2017, 17, 1132−1145

asserted that the proposed probabilistic model predicted nucleation times observed by He et al. satisfactorily. Also motivated by He et al.'s experimental results, Peters has independently suggested a similar simplified stochastic approach to predict the supersaturation of nucleation S_n in a system that is slowly supersaturated.[21] In his work, Peters emphasized that the small supersaturation approximation employed earlier in another stochastic model by Kashchiev and Firoozabadi[22] is applicable only to a special situation. In a recent study, Kadam et al. have discussed a similar probabilistic model to explain the variability in the MZW of a solute observed during crystallization with constant cooling rate.[23−25]

These theoretical approaches relate the probability of nucleation in a metastable zone to the path of the experiment using a time-dependent rate of nucleation as the variable that controls the MZW. This thought process is shared by many deterministic models as well.[26] The implication suggested by He et al.'s experiments—that a path-independent metastability boundary may exist for solutes—cannot be reconciled within the scope of these models. By appearing to predict t_n in He et al.'s experiments, the current approach adopted by many researchers suggests that the critical supersaturation observed by He et al. is of no consequence. However, He et al.'s experiments were carried out with a broad class of compounds under a wide variety of experimental conditions. Hence the possibility that a compound-specific and path-independent limit of metastability may exist for all of these materials is too intriguing to be dismissed as a simple numerical coincidence. Our present work aims to resolve this apparent contradiction and to better understand the elusive nature of the metastability limit.

In this work, we report the results from a large number of MZW experiments performed with various compounds using *isothermal solvent evaporation*. We analyze the results through the existing stochastic approach and show that this approach cannot explain the observed trends in the data satisfactorily. We discuss the possible reasons for this disagreement and then introduce a new thought process that explains the data *without relying on* a few important assumptions that underlie the current models. From this new perspective, the path-independent critical supersaturation, termed here as "induction supersaturation", can be understood as a "mean" lower boundary of the metastable zone. We conclude the discussion by emphasizing that the popular notions—(i) the MZW is a function of the rate of nucleation, and (ii) the solubility boundary is *the* lower limit of metastability—need not necessarily be correct.

2. EXPERIMENTAL SECTION

2.1. Experimental Setup. Our experiments are based on the crystallization of solutes at a constant temperature through solvent evaporation. The experimental setup used in this study was described in detail in our previous publication.[27] In summary, the setup consisted of a microfluidic crystallization platform that can hold small (5 μL) droplets of aqueous solution. These droplets were subjected to slow evaporation of solvent. The rate of evaporation was regulated by altering the geometry of the evaporation chambers. The evaporating droplets were monitored using an optical microscope, and optical micrographs of the droplets were collected once every 15 min using an automated imaging system. The time of appearance of the first crystal in the droplet was established from these images.

2.2. Methods. The experiments were performed on aqueous solutions of a wide variety of compounds including organic acids (succinic acid, adipic acid), an amino acid (L-histidine), a pharmaceutical compound (paracetamol), and a protein (hen egg-white lysozyme, HEWL). The general methods for solution preparation and handling were discussed in detail our previous publications.[19,27] All solutions were filtered through 0.2 μm syringe filters before depositing the droplets on clean silanized glass coverslips. A change in the surface characteristics of the glass coverslip did not significantly influence the outcome of the experiment.[28] Also, no crystals were observed to stick to the glass coverslip in our experiments, suggesting that crystal nucleation occurred in solution rather than on the surface. In addition, computational fluid dynamic modeling of the evaporating droplet revealed that natural convection is sufficient to ensure spatial homogeneity of the solute concentration inside the droplet, and no "drying fronts" at the edge of the droplets occur.[20] These observations lead us to believe that the sources of heterogeneous nucleation were significantly minimized in our experiments.

The experiments were conducted with various initial concentrations of solutes. We ensured that the droplets were unsaturated at the time of loading into the evaporation chambers. For hen egg-white lysozyme, the protein was buffered in a 0.1 M sodium acetate buffer at pH 4.5, and sodium chloride was used as the precipitant. The initial concentration of sodium chloride was varied such that the protein/salt ratio spanned a range of 40−100 (mg/mL)/M, where M denotes the molarity of the salt in the droplet.[27] The path of the experiment was varied by changing the initial concentration of the solute and the rate of solvent evaporation. The experimental temperatures are listed in Table 1. Almost all of our experiments resulted in the formation of a single crystal in the evaporating droplet for all the compounds studied. Rarely, a few experiments with droplets of HEWL resulted in two crystals. None of the experiments produced more than two crystals.

Table 1. Experimental Temperatures and the Corresponding Solubilities for Various Solutes Studied

compound	temperature (°C)	solubility (g/L)	reference
succinic acid	23.0	71.1	29
L-histidine	18.0	36.9	30
adipic acid	20.0	18.2	29
paracetamol	21.5	13.6	31
hen egg-white lysozyme	23.6	4.0−14.0[a]	32

[a]The solubility of hen egg-white lysozyme at the time of nucleation varies in each experiment due to an increase in concentrations of the precipitant (NaCl) and the buffer salt with time.

2.3. Estimation of Supersaturation. Typical experimental times in this study ranged from 15 to 120 h depending on the rate of evaporation of the solvent. The rates of evaporation were determined through calibration of the evaporation chambers using drying times of droplets of different compositions.[27] A mass balance model that expresses the concentration (C) of the solute as a function of time is provided in the Supporting Information. Solubility (C_{eq}) data (see Table 1) for various solutes at the experimental temperatures were obtained from respective references.[29−32] In the case of HEWL, the concentrations of both the buffer salt and the precipitant vary as the solvent (water) evaporates. This fact was taken into consideration in calculating the solubility of HEWL at any time. The supersaturation S was calculated as the ratio $S = C/C_{eq}$.

Crystal growth rates for the solutes studied, as determined from the macroscopic crystal growth experiments, are fast—on the order of 0.1 μm/s for organic solutes such as succinic acid and paracetamol,[33,34] and of 0.01 μm/s for proteins such as HEWL.[35] Under the assumption that these growth rates are independent of the size of the crystal, the time needed to grow a just-nucleated crystal to a detectable size (~5 μm) is expected to be less than the time interval between two successive images of a droplet. This expectation allows us to narrow down t_n to within 15 min. The corresponding uncertainty in the calculated S_n depends on the rate of generation of supersaturation (dS/dt) at the time of nucleation (see Supporting Information). The median uncertainty in S_n that corresponds to the 15 min uncertainty in t_n was calculated as 2.7% for succinic acid, 4.6% for L-histidine, 5.4% for adipic acid, 7.9% for paracetamol, and 9.9% for HEWL.

DOI: 10.1021/acs.cgd.6b01529
Cryst. Growth Des. 2017, 17, 1132−1145

3. RESULTS

3.1. Data Trends. While the most common technique employed in the literature in determining the MZW of compounds is cooling crystallization, our experiments used evaporative crystallization. To enable future translation of the results between the techniques, we analyze the data in terms of the driving force for nucleation. This driving force, the change in the chemical potential of the solute $\Delta\mu$ due to phase transformation, is related to the supersaturation S through the functionality $\Delta\mu = k_B T \ln(S)$, in which k_B is the Boltzmann's constant and T is the absolute temperature. Thus, one may equate the rate of change of driving force $d[\Delta\mu(t)/k_B T]/dt$ to $d[\ln(S)]/dt$. Below in Figure 1a we show S_n from our experiments as a function of $d[\ln(S)]/dt$ at the time of nucleation for succinic acid. Figure 1b depicts the same information for HEWL. For the sake of brevity, hereafter we denote the variable $d[\ln(S)]/dt$ with r and that at the time of nucleation with r_n.

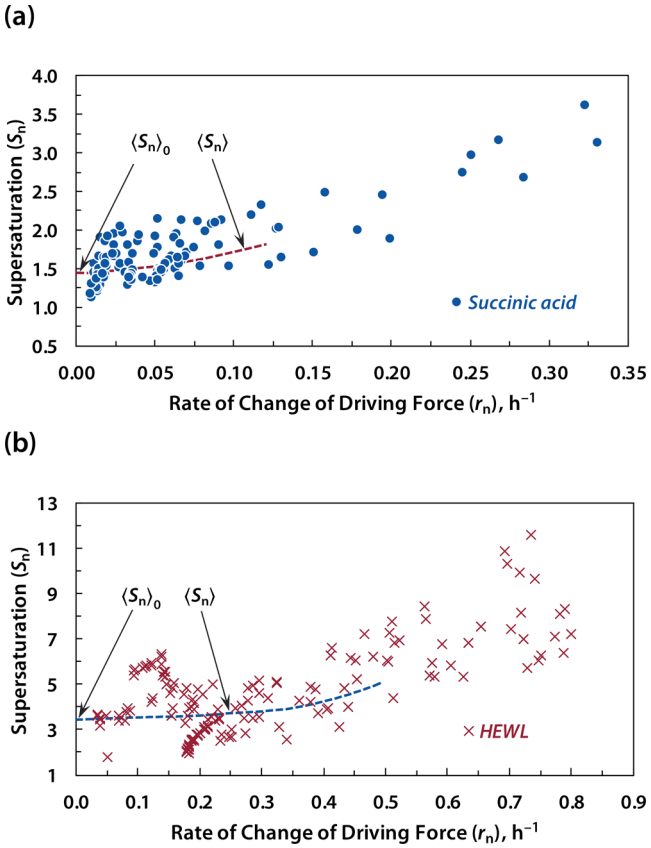

Figure 1. Plots of supersaturation of nucleation as a function of the rate of change of driving force at the time of nucleation for (a) succinic acid - 147 experiments, and (b) HEWL - 198 experiments. The dashed lines are guides to the eye to indicate the trend of an average value of S_n with varying r. As $r \to 0$, the droplets nucleated at supersaturations that are distributed around an asymptotic limiting supersaturation $\langle S_n\rangle_0$ that was well above unity.

Figure 1a,b shows that at any given r_n the observed values of S_n scatter around an average value $\langle S_n\rangle$ for both of these compounds.[36] This scatter is expected given the stochastic nature of the nucleation process. The data indicate a trend in which the average $\langle S_n\rangle$ reached in the limit of $r \to 0$, denoted here by $\langle S_n\rangle_0$, is well above unity. As r increases, $\langle S_n\rangle$ increases above $\langle S_n\rangle_0$, a result that is in general agreement with the reports from the literature. Our observations on all of the compounds studied are similar to those from succinic acid and HEWL. As with these compounds, for small values of r, a compound specific $\langle S_n\rangle_0$ that appeared to be independent of r was found for all the other solutes.

Another interesting feature exhibited by the data is that for small values of r, crystal nucleation for the compounds occurred in a *narrow band* of S_n around $\langle S_n\rangle_0$. This aspect is seen clearly from the spread of S_n around the dotted lines in Figure 1a,b. For example, in the experiments with succinic acid, when $r_n < 0.05$ h^{-1}, the resulting time required to reach S_n after crossing the solubility boundary ranged from 7 to 35 h. However, we observed no discernible variation in $\langle S_n\rangle$ for these widely spread nucleation times as shown in Figure 1a. This wide range of times to nucleation indicates the lack of a correlation between S_n and the time the droplet spent above the solubility boundary before nucleation occurred. These results emphasize the path-independent nature of S_n and suggest that when a system is slowly supersaturated, the limit of metastability may not be controlled by the time-course of the experiment.

3.2. Probability Distributions. From these observations, the data from our experiments may be classified broadly into two categories: (i) experiments at low r in which S_n appears to be path-independent and (ii) experiments at high r in which S_n is clearly affected by the path of the experiment. Figure 1a,b suggests that, when r is low, the probability of nucleation at any S may follow the same statistical distribution. Thus, the variability in S_n around $\langle S_n\rangle_0$ at low r can be used to extract information about the stochastic nature of the nucleation process. For this purpose, we define a cumulative probability of nucleation, P_s, by considering the fraction of droplets that contained a crystal by the time their supersaturation reached S.

In our experiments r increases gradually as the experiment progresses due to the nonlinear dependence of the concentration of solute on time (see Supporting Information). Any r experienced by the droplet during the course of the experiment is always lower than r_n. Hence we established a "low-r" regime for each solute by considering only the data points for which r_n is lower than a chosen cutoff value. These cutoff r_n values were chosen such that a lower cutoff did not significantly alter the distributions of P_s. Note that considering a lower cutoff may have reduced the number of data points available to construct each distribution. The chosen cutoff r_n values, along with the numbers of data points used to generate the cumulative distributions, are shown in Table 2 for each case.

Table 2. Number of Experiments and Cutoff r_n Values Used in Constructing the Cumulative Probability Distributions Shown in Figure 2

compound	number of experiments	cutoff r_n (h^{-1})
succinic acid	59	0.05
L-histidine	40	0.10
adipic acid	33	0.22
paracetamol	44	0.25
hen egg-white lysozyme	150	0.43

Figure 2 shows the statistical distributions of P_s for the five compounds—succinic acid, L-histidine, adipic acid, paracetamol, and HEWL—in the low-r regime. We remind the reader that for each compound, the data shown in Figure 2 were obtained from solution droplets that followed various time courses of supersaturation. These different paths of experiments were

DOI: 10.1021/acs.cgd.6b01529
Cryst. Growth Des. 2017, 17, 1132−1145

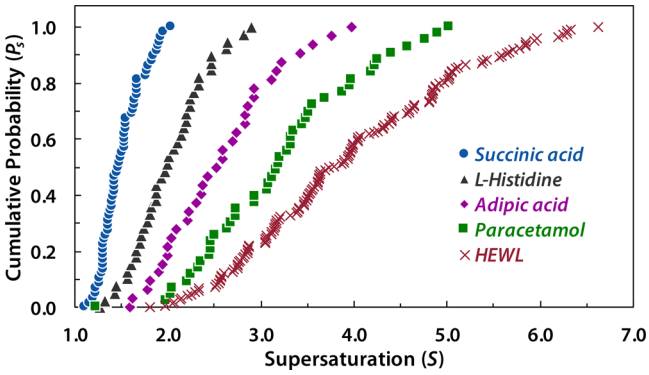

Figure 2. Cumulative probability distributions of nucleation around $\langle S_n \rangle_0$ in the low-r regime for five systems: succinic acid, L-histidine, adipic acid, paracetamol, and hen egg-white lysozyme. Each data point shown represents a separate experiment.

achieved by changing either the rate of solvent evaporation or the initial solute concentration, or both.

Three aspects are of particular interest in the data presented in Figure 2. First, the supersaturation by which about half of the drops have produced crystals (i.e., S_n at $P_s \approx 0.5$) is fairly large, ranging from ~1.5 for succinic acid to ~3.7 for hen egg-white lysozyme. These data show that, when opportunities for heterogeneous nucleation are mitigated, a crystallizing system can sustain large degrees of supersaturation without crystal formation. Second, the probability curves are compound-specific. Note that P_s was obtained from experiments in which the observed S_n was independent of r. Hence the spread for different solutes in S_n at $P_s = 0.5$ suggests that material properties must also be controlling P_s along with supersaturation, and time is not a governing factor. A third aspect of interest is that almost all of the droplets for a given compound have crystallized by the time the supersaturation reached a high value S_{max} (e.g., $S_{max} \approx 2.0$ for succinic acid and ~6.6 for hen egg-white lysozyme; see Section 4.6). This result indicates that, when the system is supersaturated slowly, a high supersaturation exists beyond which the system may not sustain metastability and nucleation becomes imminent.

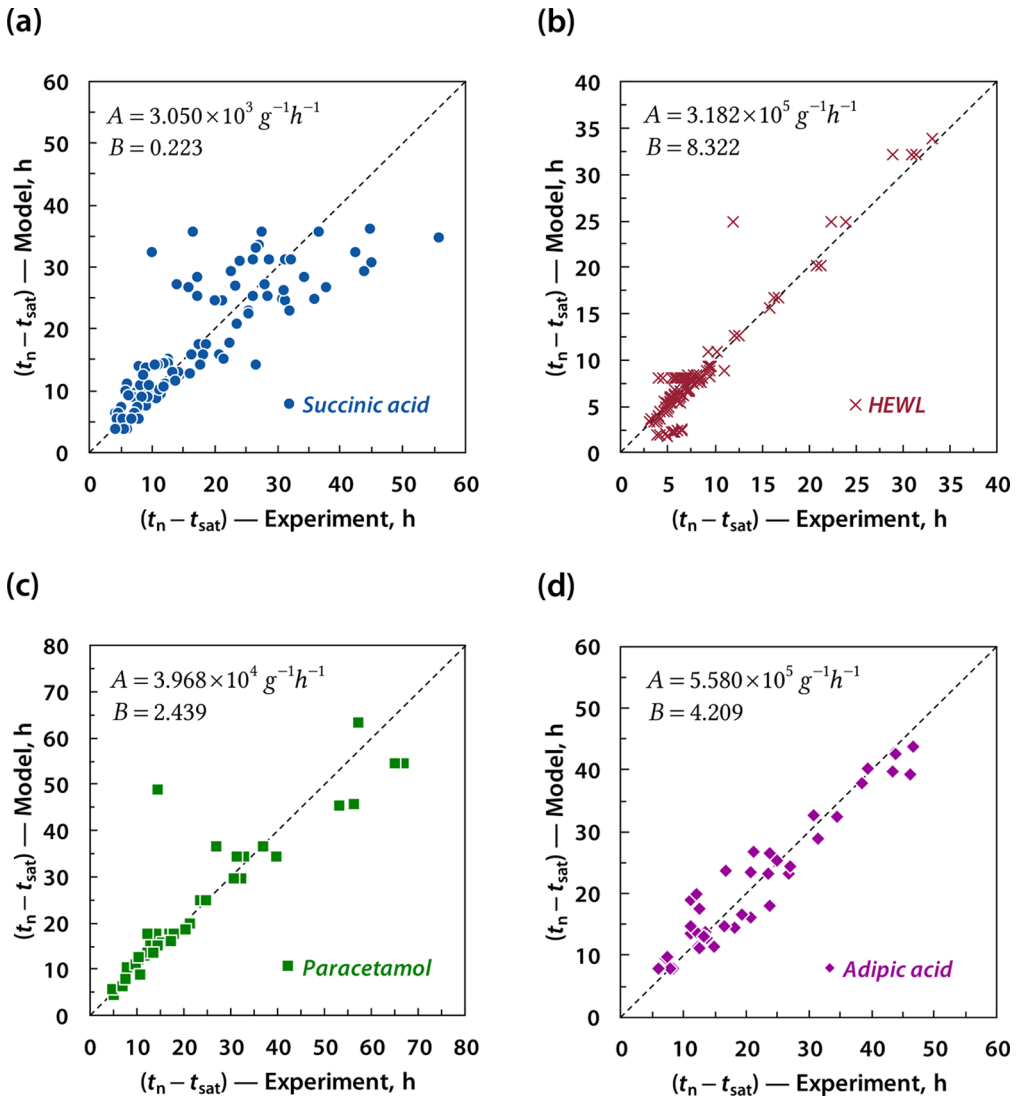

Figure 3. Comparison of $(t_n - t_{sat})$ between experimental data and model predictions for (a) succinic acid, (b) hen egg-white lysozyme, (c) paracetamol, and (d) adipic acid. Each data point shown represents a single experiment. The dotted line indicates the $Y = X$ line. The kinetic parameters A and B of eq 2 obtained from least-squares regression for each case are given in the inset of each panel.

DOI: 10.1021/acs.cgd.6b01529
Cryst. Growth Des. 2017, 17, 1132−1145

3.3. Predictions from the Existing Models. From the existing theoretical explanations, a metastable zone can only be defined with reference to the experimental path and the supersaturation dependence of the rate of nucleation.[20,21,26,37,38] This viewpoint, as interpreted by Peters,[21] leads to the conclusion that in the limiting case of very slow rates of generation of supersaturation nucleation must occur at the solubility boundary (i.e., $S_n \rightarrow 1$ as $r \rightarrow 0$). The experimental data shown in Figure 1a,b appear not to conform to this prediction. Moreover, according to these stochastic models, experiments that started from different initial conditions and followed different paths must result in different probability distributions in S_n. Again, the cumulative probability distributions of P_s shown in Figure 2, which were obtained from the spread of S_n as $r_n \rightarrow 0$ in Figure 1, are not in line with this inference.

To investigate these unexpected observations further, below we analyze the results through the predictions of the time of nucleation t_n and the supersaturation of nucleation S_n using the existing theoretical arguments. Here we follow the analysis of Goh et al.[20] because this work provides explicit expressions for the probability distributions of t_n in the evaporating microdroplet. In this model the rate of change of driving force is automatically accounted for in the $S(t)$ functionality, and no special distinction is made with respect to the effect of r on the probability of nucleation.[39] For this reason, we consider all of the data points (i.e., those from both the low-r and the high-r regimes) in the following analysis.

3.3.1. Mean Time of Nucleation (t_n). In a system with time-varying supersaturation, the stochastic formulation by Goh et al.[20] specifies the mean time of nucleation t_{mean} (defined as the mean induction time for the nucleation of at least 1 crystal in the droplet), as

$$t_{mean} = \int_0^\infty t\kappa(t) e^{-\int_{t_{sat}}^{t} \kappa(s)\, ds}\, dt \quad (1)$$

in which t denotes time, $\kappa(t)$ is the time-dependent rate of nucleation in the entire system, and t_{sat} is the time at which the system has reached the solubility boundary during the gradual increase of driving force. The nucleation rate $\kappa(t)$ in the system with a time-dependent volume $V(t)$ is considered to be given by the product $J(t)V(t)$, where $J(t)$ is the steady-state rate of nucleation per unit volume of solution. $J(t)$ is expressed through a phenomenological equation such as

$$J(t) = AC(t) \exp\{-B/\ln^2[S(t)]\} \quad (2)$$

Equation 2 is based on the classical nucleation theory (CNT).[40] CNT expresses the steady-state rate of nucleation through a combination of a kinetic pre-exponential factor A, the solute concentration $C(t)$, and the normalized energy barrier to nucleation $B/\ln^2[S(t)]$ with B being a compound-specific parameter and $S(t)$ being the time functionality of supersaturation.

In line with the analysis of Goh et al., here we treat the time of nucleation t_n from each experiment as equivalent to t_{mean} expressed through eq 1. Since no nucleation occurs until the droplet crosses the solubility boundary, we consider the lower limit of all integrations in eq 1 to be given by t_{sat}. Using the least-squares procedure outlined by Goh et al., we find the values of A and B that best describe the data obtained on various systems. If the model represents the experimental system well, one should be able to obtain a unique set of A and B that matches t_n with t_{mean} for all data points with minimal error.

Figure 3a–d shows the predictions of t_n from eq 1 used in combination with eq 2. Parameters A and B found from the least-squares regression are shown in the insets. In these figures, the time the droplets spent after crossing the solubility boundary, $(t_n - t_{sat})$, was compared between the experiments and the model. One may consider that the model predictions agree well with the experimental data for paracetamol and hen egg-white lysozyme for many data points, but for not all of them. The agreement for adipic acid is fair. Usually, in the literature, the quality of fits similar to those shown in Figure 3b,c is taken as a confirmation that the underlying theory describes crystal nucleation in a metastable zone satisfactorily. On the basis of such plots, literature reports typically assert that the width of the metastable zone is a function of the rate of nucleation through eq 1. However, the poor quality of the fit seen in Figure 3a for succinic acid raises concerns regarding this traditional argument.

In the literature, disagreements as seen in Figure 3a are usually attributed to the inaccuracy in the nucleation kinetics information employed by the model. For example, Chen et al. have attempted to explain the observed disagreements in glycine nucleation times by considering the possibility of a non-monotonic variation of the rate of nucleation with time.[41] These authors have argued that when nucleation follows a nonclassical pathway (e.g., a pathway consisting of two-step nucleation[42]), then eq 1 may not describe the time of nucleation when the rate of nucleation is considered to be given by eq 2. While such possibilities cannot be discounted, as we discuss below, a simpler explanation may be provided for the observed disagreements by critically examining the origins of eq 1.

Below we show that the disagreements between the model and data are too systematic to be attributable to inaccurate nucleation rate parameters. The following analysis highlights that the "excellent agreement" between the model and the experiment, perceived in terms of the time of nucleation (t_n), may not necessarily exist when one compares the model predictions in an alternate coordinate space of the supersaturation of nucleation (S_n).

3.3.2. Mean Supersaturation of Nucleation (S_n). During a metastable zone experiment, one is primarily interested in the average supersaturation of the system at which nucleation occurs. The stochastic approach used in deriving eq 1 specifies this mean supersaturation only in reference to the path of the experiment, i.e., the mean supersaturation of nucleation S_{mean} is simply the supersaturation experienced by the system at t_{mean}. In Figure 4a–d we compare S_{mean} in our experiments (= S_n @ t_n) to S_{mean} @ t_{mean} obtained from the model.

A systematic deviation between the predictions of the model and the experimental data emerges as one examines Figure 4a–d. In fact, one finds no correlation between the experimental data and the predicted values of S_n for any compound! For example, for succinic acid (Figure 4a), regardless of the initial conditions of the experiment, the model never predicts nucleation to occur earlier than a time that corresponds to a supersaturation of 1.4. But experimentally we see that nucleation occurred anywhere between S_n = 1.1 to 3.5 with no discernible pattern. This disagreement cannot be attributed to the possible uncertainty in the experimental S_n, which is only about 3% for this case. Similar trends in the data are seen for other compounds.

The calculations of both S_n from t_n (experimental) and S_{mean} from t_{mean} (model) use the same information on the path of the experiment, i.e., the same $S(t)$ functionality. Yet, one sees no correlation between the predicted S_{mean} and the actual S_n for any solute. This observation indicates that any agreement seen in the

DOI: 10.1021/acs.cgd.6b01529
Cryst. Growth Des. 2017, 17, 1132–1145

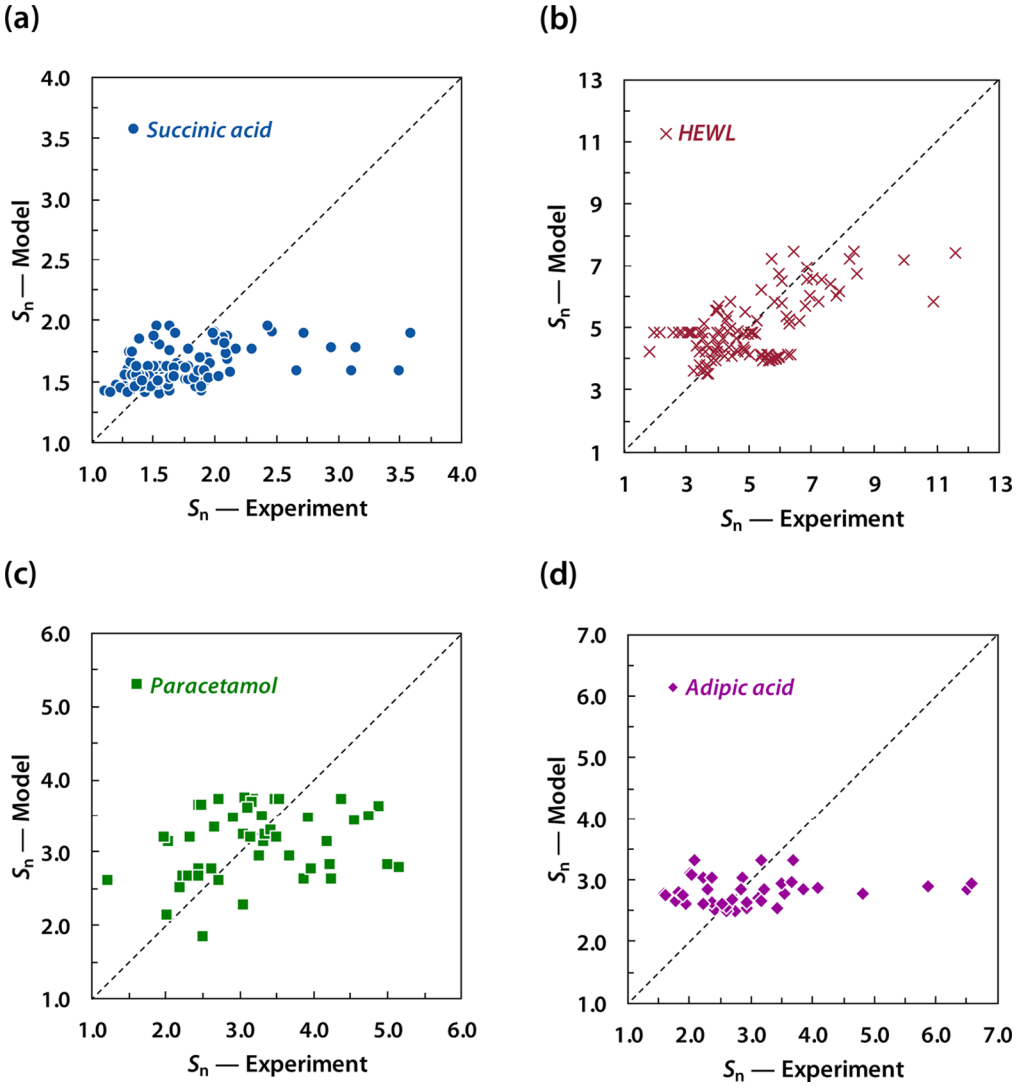

Figure 4. Comparison of S_n between the experimental data and the model predictions for (a) succinic acid, (b) hen egg-white lysozyme, (c) paracetamol, and (d) adipic acid. Each data point shown represents a single experiment. The dotted line indicates the $Y = X$ line. The kinetic parameters A and B of eq 2 used for each case are given in Figure 3, panels a–d, respectively.

time comparisons (Figure 3a–d) is fortuitous. In other words, the seemingly minor differences between the predicted t_{mean} and the experimental t_n in reality are very significant in terms of the supersaturation at nucleation. Figure 4a–d strongly suggests that somehow the widely used theoretical approach to model nucleation in a metastable zone is unable to capture the physics of the process through eq 1. The discussion below focuses on identifying the cause of the disagreement seen in Figure 4a–d through a critical examination of the development of the stochastic model.

4. DISCUSSION

4.1. The Stochastic Formulation. The mean time of nucleation t_{mean} given by eq 1 represents a probability density function (PDF) $f(t)$ defined by[20]

$$f(t) = \kappa(t)e^{-\int_{t_{sat}}^{t} \kappa(s)\,ds} \tag{3}$$

in which the variables are as defined in eq 1. Equation 3 specifies the probability for nucleation to occur within an infinitesimal time interval dt of t, i.e., in a time interval $(t, t + dt)$. The corresponding cumulative distribution function (CDF) for the droplet to contain *at least* one nucleus by a time t, $F(t)$, is

$$F(t) = 1 - e^{-\int_{t_{sat}}^{t} \kappa(s)\,ds} \tag{4}$$

Equations 3 and 4 are derived through the survival probability analysis of a nucleating system. In this thought process, the formation of a single nucleus represents a *transition* in the *state* of the system from having one less nucleus to having current number of nuclei. The time evolution of probabilities for such transitions are captured by the Master equation[20,43] as a set of ordinary differential equations given by

$$\frac{dP_0(t)}{dt} = -\kappa(t)P_0(t), \quad P_0(0) = 1 \tag{5}$$

$$\frac{dP_n(t)}{dt} = -\kappa(t)[P_{n-1}(t) - P_n(t)], \quad P_n(0) = 0, n = 1, 2, \ldots \tag{6}$$

in which $P_n(t)$ represents the time evolution of the probability that a system contains n nuclei. These differential equations

DOI: 10.1021/acs.cgd.6b01529
Cryst. Growth Des. 2017, 17, 1132–1145

represent a particulate process described as a nonstationary Poisson process.

This description of the time evolution of a stochastic system is based on the theorems of stochastic process analysis which find applications in the solution of several fundamental problems, such as the study of Brownian motion.[43] Central to the application of the general stochastic theoretical framework to the nucleation problem is the *premise* that the probability of nucleation in an infinitesimal time interval dt is given by $\kappa(t)$ dt in which $\kappa(t)$ is the time-dependent rate of nucleation in the *entire* system. Below in Sections 4.2 and 4.3 we visit the origins of this premise and examine its validity in different scenarios. To avoid digression, here we discuss these concepts only in brief. We emphasize that a comprehension of the probabilistic relevance of the nucleation rate is essential for understanding the central idea of this paper. A more detailed discussion on the development of the stochastic analysis of nucleation is provided in the Supporting Information.

4.2. Probabilistic Relevance of Nucleation Rate. Theoretical descriptions of nucleation hypothesize that a system must cross a free energy barrier for nucleation to occur.[40] Successful nucleation occurs when a cluster of a critical size, the *critical cluster*, forms in the solution and grows further. The stochastic approach to modeling nucleation through the Master equation considers nucleation as a Markov process[43,44] in which density fluctuations of various magnitudes occur in a solution *spontaneously*. The phrase "probability of nucleation" essentially refers to a probability p that a *critical* density fluctuation occurs spontaneously in the system, because that is the true "chance event" in this context.[45] Hence, in the probabilistic viewpoint, the formation of a nucleus is treated as a rare success among many random attempts made by the system to cross the energy barrier. In this context, the rare "success" is the occurrence of a density fluctuation of the *critical size*, and the random "attempts" are the density fluctuations of *various sizes* that occur spontaneously. Within the scope of the Markov approximation, these attempts are considered to occur *one after another* in time. This viewpoint then allows one to define a relation between time and the probability of nucleation.

The Markov description of nucleation concerns the probability of a transition in the system from a state of having n nuclei to that of having $(n + 1)$ nuclei (hereafter simply referred to as an $n \rightarrow (n + 1)$ transition). The attempts toward this transition are *hypothesized* to occur at an *attempt frequency* ν, with a probability of success p for each attempt. Statistical mechanics considerations suggest p to be given by the Boltzmann distribution law as[40,46,47]

$$p = \exp(-\Delta G^*/k_B T) \tag{7}$$

in which ΔG^* is the change in the Gibbs free energy associated with the formation of the critical cluster (i.e., the energy barrier to nucleation). The hypothetical attempt frequency ν, however, is meant to be obtained from experimental data.[48] From eq 7, one notes that the success probability p for an $n \rightarrow (n + 1)$ transition to occur *in a single attempt* depends only on the prevailing energy barrier, and not on time. On the other hand, the *transition* probability that the system will have an $n \rightarrow (n + 1)$ transition in a unit of time is obtained by *defining* a rate of change of transition probability κ. In other words, one formulates a *time-continuous* description of nucleation mediated through *discrete* density fluctuations through the definition of κ.

The premise that the rate of transition probability κ is given by the rate of nucleation JV originates from the Markov analysis of nucleation *at a constant supersaturation* (induction time experiment). When the supersaturation does not vary with time, p is independent of time and is not expected to change in between the *successive* attempts (density fluctuations). The hypothetical attempt frequency ν implies that time in the system should evolve in blocks of $(1/\nu)$ units through the occurrence of *successive* density fluctuations. This construct, coupled with the fact that p remains constant during the time interval $(1/\nu)$, allows one to define a κ that bridges the time gap between two successive density fluctuations as $\kappa = p/(1/\nu) = \nu p$. Subsequent mathematical manipulation to relate the probability to time involves solution of the Master equation similar to eq 6 for the case of constant supersaturation (time-independent κ). The resulting solution provides a CDF for the probability of nucleation as a function of time as[20]

$$F(t) = 1 - e^{-\kappa t} = 1 - e^{-(\nu p)t} \tag{8}$$

Equation 8 represents the CDF of a stationary Poisson process with a Poisson rate parameter of κ. Hence the Markovian model is also referred to as the Poisson model of nucleation.

The quantity $\kappa = \nu p$, by definition, implies that the probability of an $n \rightarrow (n + 1)$ transition reaches unity in $(1/\nu p)$ time units. This definition may be interpreted as νp to be the rate at which the system *on the whole* produces individual nuclei one after another. In this sense $\kappa = \nu p$ holds the meaning as the steady-state rate of nucleation for a system producing successive density fluctuations at a constant supersaturation. Equation 8 thus provides the *stochastic definition* of the nucleation rate κ.

The Poisson description of nucleation, which considers the spontaneous occurrence of density fluctuations that bring *several molecules together at once* randomly, is very different from a mechanistic description of CNT, which describes nucleation to occur through the attachment/detachment of *monomers* with prescribed rates to a growing population of clusters. Historically, the link between the probabilistic (Poisson) and the deterministic (CNT) viewpoints of nucleation is achieved through the manipulation of the variables ν, p, and the system volume V together to conveniently *define* a new variable J that can be interpreted as the nucleation rate provided by the mechanistic (CNT) arguments.[48] Since νp holds the meaning of a stochastic nucleation rate in the entire volume of the system V, one writes a nucleation rate *per unit volume* J as $J = (\nu/V)p = J_0 \exp(-\Delta G^*/k_B T)$ in a form that is similar to the "deterministic" nucleation rate given by the CNT. The pre-exponential factor J_0 from the CNT rate expression now has a physical relevance to the probabilistic viewpoint as the number of density fluctuations (of any size) the system can produce per unit volume per unit time.

From the above discussion, one notes that the central premise of the stochastic analysis, that the probability of nucleation in the time interval dt is given by κ dt (with $\kappa = JV$), originates from the Markov analysis of the system nucleating *at a constant supersaturation*. Note that the nucleation rate J from the CNT is related to the probability of nucleation only *ex post facto*,[48] through the equality $\nu p = JV$. Equation 8 thus *redefines* the nucleation rate from the CNT as an "average" rate that can be used to predict the probability of nucleation. However, this equation itself does not originate from the CNT.

Furthermore, within the scope of the stochastic model, the probability of nucleation is primarily a function of time only through the hypothetical attempt frequency ν and *not* through the rate of nucleation J. The nucleation rate J is simply a redefinition of the product νp per unit volume to assimilate the mechanistic (CNT) viewpoint of nucleation into the proba-

DOI: 10.1021/acs.cgd.6b01529
Cryst. Growth Des. 2017, 17, 1132−1145

bilistic viewpoint. This distinction is often not emphasized in the published literature, leading to an inadvertent and incorrect interpretation that the probability of nucleation is a function of time because of the existence of a nucleation rate in the CNT sense. The reader may wish to consult the Supporting Information for further elaboration of the thought process behind eq 8.

4.3. Assumptions Used in the Markov Analysis of Nucleation. The following assumptions are employed in deriving eqs 5 and 6, and also eq 8:[43]

(i) *The One-Step Assumption*. The Markovian description of nucleation assumes that only transitions (jumps) between successive number of nuclei are *probable*; i.e., the system can only transition from having n nuclei to having $n + 1$ nuclei in an infinitesimal time interval dt. The probability of a jump that skips states (such as n nuclei to $n + 2$ nuclei) within dt is considered to be extremely small and is neglected.

(ii) *The Stationarity Assumption*. All $n \rightarrow (n + 1)$ transitions occur at the same rate that is independent of n. Also, one assumes that no $n \rightarrow (n - 1)$ transitions occur; i.e., once a nucleus forms, it stays in solution.

(iii) *The Repeated Randomness Assumption (Stosszahlansatz)*. The infinitesimal time interval dt is long enough for the system to equilibrate to the process conditions at t, and the equilibrium distribution of the microscopic variables at t + dt depends only on the state of the system at t. Hence the differential limit d$t \rightarrow 0$ should not be interpreted literally to mean d$t = 0$.

(iv) *The Linearity Assumption*. The probability of an $n \rightarrow (n + 1)$ transition changes linearly with time at a rate κ during dt. In other words, this rate κ remains constant during dt, but may change in adjacent dt intervals. This assumption implies that the time "unit" on which the "rate" κ is defined is smaller than the time interval dt, i.e., dt consists of multiple time units, with each unit of time defined in such a manner that the discrete evolution of the process can be approximated by a time-continuous description.

Despite its rigorous appearance, the Markov analysis that underpins the derivation of eqs 5 and 6 and 8 is only *an approximation* of the nucleation process that relies on the validity of the above well-defined assumptions. At constant supersaturation, successive density fluctuations in the system occur at the same supersaturation. For this case a rate of transition probability κ over a coarse-grain time unit that spans multiple density fluctuations can be defined with a physical meaning without violating these assumptions. *However, when one extends the same logic to analyze nucleation under time-varying supersaturation, contradictions arise*!

4.4. Markov Analysis of an MZW Experiment – Inconsistencies. Let us look at the validity of the above assumptions for the Markov analysis of nucleation under *time-varying* supersaturation (i.e., for the case of a metastable zone experiment). *By definition*, in an MZW experiment the supersaturation of the system continuously increases as specified by $S(t)$. The *one-step* assumption of a Markov jump process mandates a nucleation mechanism that proceeds through discrete density fluctuations that occur one after another. From the *repeated randomness* assumption, the system must be equilibrated to $S(t)$ at any time t. These two Markovian assumptions, together with the experimental requirement of a continuous $S(t)$, logically dictate that the system must experience each density fluctuation at a different supersaturation. Note that the CNT viewpoint of J as a measure of steady-state flux of nuclei has no relevance here. For a stochastic description of nucleation process, one needs to consider the probabilistic (attempt-success) perspective of nucleation, not the mechanistic (steady-state cluster population) viewpoint. Time in the experiment evolves through the occurrence of nonsimultaneous density fluctuations.

The assumption on the *linearity of the rate of transition* stipulates that during the infinitesimal time interval dt that follows a certain time t, the rate of change of transition probability $\kappa(t)$ must remain constant. When one assumes that $\kappa(t)$ is given by the nucleation rate in the system at t, i.e., $\kappa(t) = J(t)V(t)$, one implicitly has also assumed that the system experiences successive density fluctuations at a frequency of ν (= J_0V). In other words, one has already assumed that time evolves in steps of $(1/\nu)$ units. Thus, any two density fluctuations that occur one after another must occur at two different supersaturations $S(t)$ and $S(t + 1/\nu)$. As a result, the linear rate (constant-$\kappa(t)$) assumption is valid only for the duration between two successive density fluctuations, $(1/\nu)$, and any dt considered should be less than $(1/\nu)$ units of time.

For a transition (success) to occur under the assumed physical process, a density fluctuation (attempt) must occur. By definition, *no* attempts occur in between two *successive* density fluctuations, and hence *no physical mechanism exists* to generate a transition during a d$t < 1/\nu$. Hence, the rate of change of transition probability must be zero for this duration. In other words, when the supersaturation is continuously varied, $\kappa(t)$ must be zero during any physically meaningful dt. As a result, when one considers the supersaturation to vary continuously with time, $P_n(t)$ (see Section 4.1) cannot evolve on a fine-grain time scale in between two successive density fluctuations, i.e., during any dt one may consider. This conclusion makes a Markov description of the process impossible and renders eqs 5 and 6 invalid.

Thus, one notes that a Markovian analysis of a metastable zone experiment cannot be formulated logically using the necessary assumptions. Regardless of the subtle contradictions, if one proceeds anyway with the Master equation approach (eqs 5 and 6) by considering $\kappa(t) = J(t)V(t)$, such an analysis is not in line with the assumed physical description of the process. To ensure a continuous-time description of a discrete process that evolves in time in steps of $(1/\nu)$ time units, the mathematical formulation that considers $\kappa(t) = J(t)V(t)$ incorrectly decreases $P_n(t)$ and increases $P_{n+1}(t)$ during a time step. This is so because, in such a formulation, despite the physical impossibility, a transition is considered probable in the time interval between two density fluctuations. The time interval dt is treated conceptually by eqs 5 and 6 as if multiple density fluctuations occur at $S(t)$, whereas only one density fluctuation should be counted in the analysis. The integration of $J(t)V(t)$ over the path of the experiment, as implemented in solving eqs 5 and 6, thus incorrectly represents the physical process. Such integration artificially inflates the probability of nucleation on a continuous time axis and predicts nucleation to occur with an appreciable probability at a much lower supersaturation than otherwise. This inflation of probability is clearly seen in Figure 4a–d, in which the model-predicted range of S_n (vertical spread of data) is always narrower than the experimentally obtained range (horizontal spread).

In summary, the disagreement shown in Figure 4a–d originates from an incorrect representation of the physical process by the stochastic model brought forth by the use of nucleation rate to represent the rate of transition probability of the system. This approach presupposes the validity of the assumptions on which the equality of $\kappa = JV$ is founded for the

DOI: 10.1021/acs.cgd.6b01529
Cryst. Growth Des. 2017, 17, 1132–1145

case of nucleation in the metastable zone. In light of the above discussion, to capture the observed trends in the experimental data, one realizes that one needs a *better approximation* of the process than the (incorrect) Markov description that relies on the use of a nucleation rate. Below we develop such a thought process that leads us to interesting conclusions.

4.5. Nucleation in a Metastable Zone – New Approach. Density fluctuations are random in time in that a density fluctuation can occur spontaneously at any time in a system. This unpredictability of the occurrence of a fluctuation is the reason why nucleation is stochastic in the first place. At *constant supersaturation*, the randomness in the time of nucleation arises in part from the uncertainty in the time at which the next density fluctuation (attempt) will occur.[49] For the same reason, when the supersaturation of the system is varied continuously, the *supersaturation* at which the "next" density fluctuation occurs is also uncertain. In the constant-supersaturation case, the uncertainty in nucleation time is tackled by introducing a hypothetical attempt frequency ν. This construct allowed one to *define* a nucleation rate J as $(\nu p/V)$. Such a presumed attempt frequency ν dictates time t to evolve in steps of $(1/\nu)$. For the case of a time-varying supersaturation, however, this construct mandates that the system should make successive attempts only at "predetermined" supersaturations (i.e., at $S(t)$, $S(t + 1/\nu)$, $S(t + 2/\nu)$, etc.). Thus, a "path dependency" of the process is automatically introduced into the mathematical formulation through the use of a nucleation rate, and the process can no longer be considered stochastic.

Hence, to preserve the randomness involved in the occurrence of the "next" density fluctuation, one would rather *not* make an assumption regarding the attempt frequency. However, without the concept of an attempt frequency, the question one faces is how can one establish the continuity of time. Fortunately, the specified supersaturation path $S(t)$ is an independent variable that is controlled by the experimenter, and a one-to-one correspondence exists between time t and supersaturation $S(t)$. Thus, one may contemplate representing the evolution of time in the MZW experiment indirectly through $S(t)$ and the evolution of probability of nucleation through the functionality $p(S)$.

4.5.1. Energy Barrier As the Primary Variable. The problem of predicting $f(t)$ in an MZW experiment greatly simplifies when one considers the energy barrier to nucleation as the primary variable. In a metastable zone experiment that starts from a saturation condition, the energy barrier $(\Delta G^*/k_BT)$ is gradually lowered from being infinite to being an energy barrier at which nucleation is observed. To facilitate the following discussion, first let us define a new random variable g as

$$g \equiv (\Delta G^*/k_BT) \tag{9}$$

The energy barrier is a monotonic function of supersaturation. Hence a one-to-one correspondence exists between the energy barrier g and time t through $S(t)$. Any time interval $(t, t + dt)$ may be represented by a unique energy barrier interval $(g, g + dg)$.

Considering the energy barrier interval instead of the time interval has other advantages. First, the randomness of a density fluctuation to occur at any *time* between the two energy barriers g and $(g + dg)$ is preserved. Second, if the rate of change of energy barrier is large, the assumption that the system is equilibrated to the prevailing energy barrier during dt may not hold. Instead, when an infinitesimal energy barrier interval is considered, then not only the corresponding time interval dt is infinitesimal, but also one's assumption that the system equilibrates to the prevailing supersaturation is more reasonable. Thus, to capture the true stochastic nature of the density fluctuations, we consider density fluctuations to occur *randomly* in the energy barrier (supersaturation) space and associate the successive density fluctuations to the passage of time through $g(t)$.

4.5.2. Probability Functions for MZW. When a system experiences an energy barrier g, the probability that a spontaneous critical density fluctuation occurs is given by p as $p(g) = \exp(-g)$ (eq 7). When the energy barrier is *continuously* varied, p may be interpreted as the probability of success for a single density fluctuation that *may randomly occur* in the energy barrier interval $(g, g + dg)$. In that sense, we interpret eq 7 as a function that expresses the probability density of nucleation at g and write the PDF as

$$f(g) \equiv p(g) = \exp(-g) \tag{10}$$

Equation 10 is an exponential distribution function with a characteristic "rate parameter" of unity. Hence it is suitable to represent a Poisson process of nucleation in which a density fluctuation that occurs at a certain energy barrier g_1 has no influence over that at a subsequent energy barrier g_2. Following this line of thought, we express the CDF for at least one critical nucleus to form while the energy barrier is lowered from $g = \infty$ (at $S = 1$) to a certain g (at S) as

$$F(g) = \Pr(g_n \geq g) = \int_{\infty}^{g} \exp(-g')\, dg' = -e^{-g} \tag{11}$$

in which g' is the dummy variable of integration. With the progress of the experiment, as time *increases*, the energy barrier *decreases*. The negative sign in front of the exponential in eq 11 reflects this fact and hence can be ignored. This inverse relationship between g and t is also implied in the definition of the cumulative probability as $F(g) = \Pr(g_n \geq g)$ instead of the conventional $F(t) = \Pr(T_n \leq t)$ where T_n is the time of nucleation. Note that $F(g)$ represents the cumulative probability of nucleation in the system by a time $t = g^{-1}(g)$ where g^{-1} represents the inverse functionality corresponding to $g(t)$. In the following section, we examine the effectiveness of eq 11 in capturing the experimental probability distributions shown in Figure 2.

4.6. MZW as a Function of Supersaturation. Using eq 11, we have related the probability of nucleation in a continuously supersaturated system to the energy barrier through a simple exponential function. To evaluate the utility of eq 11 in predicting the probability of nucleation at any S_n, we now need a method to link g to S that facilitates a translation of $F(g)$ into the quantity P_s discussed in the context of Figure 2. The energy barrier to nucleation at a given supersaturation can be estimated through several approaches, such as CNT,[40,50] density functional theory (DFT),[51,52] and rigorous computational methods.[47,53] Below we use the CNT approach to evaluate the energy barrier and compare the predictions from eq 11 with the experimental data.

Within the scope of the classical nucleation theory, the capillarity approximation for a spherical nucleus expresses the energy barrier g through the reversible work of formation of a spherical critical cluster, W^*, as[40]

$$g \equiv (W^*/k_BT) = (4\pi^3\Gamma^3)/(27 \ln^2 S) \tag{12}$$

In the above equation, the dimensionless interfacial free energy Γ between the cluster and the solution is defined as $\Gamma = (\gamma d^2/k_BT)$ in which d is the solute molecular diameter and γ is the energy involved in the creation of a unit area of the new crystal surface within the solvent.

DOI: 10.1021/acs.cgd.6b01529
Cryst. Growth Des. 2017, 17, 1132−1145

Now let us consider S_{max} (for the definition of S_{max} see Section 3.2). For eq 11 to capture the observed limiting behavior of $P_s \rightarrow 1$ as $S_n \rightarrow S_{max}$ (Figure 2), S_{max} should be a supersaturation at which g vanishes. Mean-field theoretical arguments suggest that the energy barrier to nucleation vanishes at the spinodal concentration.[50,54,55] That eq 12 does not vanish as the solute concentration approaches the spinodal concentration is a known shortcoming of the CNT formulation. To circumvent this limitation in the context of eq 11, we ask the following question: within the scope of CNT, at what cluster size should the energy barrier to nucleation become so low that nucleation becomes imminent (i.e., $P_s \rightarrow 1$)? One may contemplate that when the system reaches a high degree of supersaturation at which the number of molecules in a critical nucleus (ζ^*) becomes unity, nucleation should become *effectively* barrier-free. Note that we are not suggesting that the critical cluster size (ζ^*) drops to a single molecule at the spinodal concentration. We are merely emphasizing the fact that for $\zeta^* < 1$, the CNT formulation loses its physical significance. If the CNT were to somehow successfully capture a vanishing energy barrier, a meaningful location for it should be at a supersaturation at which $\zeta^* = 1$. From this perspective, to capture the observed trends in the data within the scope of eq 11, we hypothesize the following correction for the energy barrier given by eq 12, which will force g to approach zero as $S_n \rightarrow S_{max}$.

CNT provides the relationship between the number of molecules in a spherical critical cluster, ζ^*, and the supersaturation S, as[40]

$$\zeta^* = (8\pi^3\Gamma^3)/(27 \ln^3 S) \quad (13)$$

By equating ζ^* to 1, we obtain S_{max} from eq 13 as $\exp(2\pi\Gamma/3)$, and using this value in eq 12, g at $\zeta^* = 1$ as

$$g|_{\zeta^*=1} = (W_1/k_BT) = (\pi\Gamma/3) \quad (14)$$

in which W_1 represents the reversible work of formation of a critical cluster that contains a single molecule. By subtracting (W_1/k_BT) from the energy barrier given by eq 12, we define a "corrected" energy barrier that vanishes as $S_n \rightarrow S_{max}$. Using this corrected energy barrier, we now express $F(g)$ in terms of supersaturation S, and obtain P_s, the cumulative probability of nucleation in a metastable zone, as a function of S, as

$$P_s = \exp\left(-\frac{W^* - W_1}{k_BT}\right) = \exp\left(\frac{\pi\Gamma}{3} - \frac{4\pi^3}{27}\frac{\Gamma^3}{\ln^2 S}\right) \quad (15)$$

The distributions of P_s predicted by eq 15 for the solutes studied are shown in Figure 5. The agreement between the model and the experimental data is highly satisfactory. The values of Γ obtained by curve-fitting for the compounds studied are given in Table 3. Table 3 also gives the interfacial free energies in their dimensional form (γ).

The values of γ reported in the literature for various solutes vary widely depending on experimental techniques and theoretical arguments employed in those studies. Nevertheless, the interfacial free energies obtained from our data through eq 15 are comparable to those reported in the literature. For example, Granberg et al. suggested the values of γ for paracetamol to range from 1.8 to 4.7 mJ/m^2 depending on the experimental technique used.[56] The value we obtained for paracetamol (7.1 mJ/m^2) is in the vicinity of this range. For HEWL, using induction time measurements, Kulkarni et al. have obtained Γ values in the range of 0.87−1.80 (corresponding to a γ range of 0.39−0.81 mJ/m^2).[57] A Γ value of 0.854 we report is again close to this range. In performing such comparisons on the interfacial free energy parameters, however, one needs to be cautious. The values of γ obtained from MZW experiments that use cooling crystallization should not be compared with the γ values from our experiments. This is because such studies typically use the argument behind eqs 5 and 6 to determine the rate parameters from the MZW data. As we have shown earlier, this rate approach to MZW relies on assumptions that have questionable validity and is likely to result in erroneous determination of the nucleation kinetic parameters. Also, the interfacial free energy is expected to be correlated to the solubility of a compound through intermolecular interactions.[58,59] Thus, one expects different values of γ to result from isothermal experiments conducted at different solubilities.

From Figure 5 we show that the nucleation probability of a compound at any supersaturation under slowly increasing driving force ($r \rightarrow 0$) can be predicted using the framework of the CNT with a single parameter Γ, without a need to consider a rate of nucleation. As seen from this figure, eq 15 not only captures the aspect that $P_s \rightarrow 1$ as $S_n \rightarrow S_{max}$ (by design), it also predicts the intermediate values of P_s very well from $S_n = 1$ to $S_n = S_{max}$. The intermediate values of P_s have no connection to the used approximation of S_{max} to occur at $\zeta^* = 1$. Also, the interfacial free energy parameters obtained from the data using eq 15 are physically meaningful and are comparable to the literature values. Thus, the agreement between eq 15 and the experimental probability distributions over the entire range of S_n emphasizes the validity of the model.

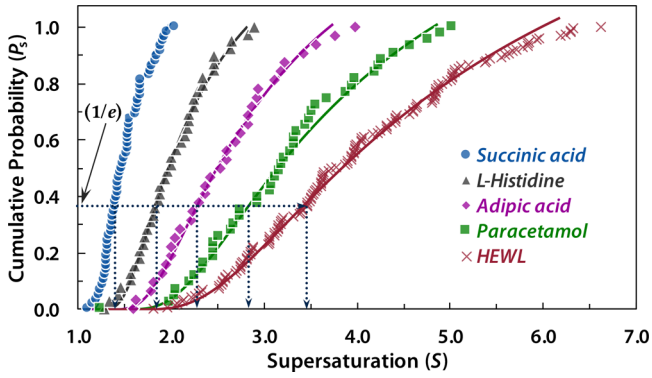

Figure 5. Cumulative probability distributions of nucleation around $\langle S_n \rangle_0$ in the limit of $r \rightarrow 0$ for five solutes: succinic acid, L-histidine, adipic acid, paracetamol, and hen egg-white lysozyme. The solid lines drawn are the predictions from eq 15. The Γ values that best fit the data for each compound are given in Table 3. The dotted lines indicate the induction supersaturations (see Section 4.8) at which P_s equals (1/e) for respective solutes.

Table 3. Maximum Experimentally Observed Supersaturation (S_{max}) at Which the Nucleation Probability P_s Approaches Unity as $r \rightarrow 0$[a]

compound	S_{max}	Γ	γ	ψ
succinic acid	2.04	0.323	4.161	1.41
L-histidine	2.90	0.494	4.976	1.83
adipic acid	4.20	0.640	6.474	2.34
paracetamol	5.02	0.749	7.104	2.83
hen egg-white lysozyme	6.62	0.854	0.383	3.42

[a]Also given are the interfacial free energy parameters (Γ and γ) that best describe the data using eq 15, and the induction supersaturation (ψ), for each compound. The units of γ are (mJ/m^2).

DOI: 10.1021/acs.cgd.6b01529
Cryst. Growth Des. 2017, 17, 1132−1145

4.7. S_{max} and the Corrected Energy Barrier. A few aspects of eq 15 merit further discussion. The corrected energy barrier $(W^* - W_1)/k_BT$ has been discussed in the literature in the context of equilibrium cluster size distribution (CSD) function.[40] This term naturally appears in the derivation of an expression for a self-consistent equilibrium CSD that satisfies the law of mass action.[60,61] The observation that this corrected energy barrier may be used to predict the probability distribution of the metastable zone width (S_n) from energetic considerations alone is an interesting result from the present work. Even though eq 15 agrees very well with experimental data for all the compounds studied, we note that the model increasingly overpredicts P_s as $S_n \rightarrow S_{max}$, alerting us to the fact that the corrected energy barrier was forced to vanish at $\zeta^* = 1$, and S_{max} for each compound may or may not represent a true spinodal concentration.

Within the context of the CNT, we have speculated that S_{max} may correspond to a supersaturation at which the number of molecules in a critical nucleus becomes unity. On a cursory read this *speculation* may appear to the reader as a *trivial conclusion* drawn by us that the spinodal should occur at a supersaturation at which $\zeta^* = 1$. We emphasize that this is not our conclusion. The existence and the nature of S_{max} are highly interesting. We mention here that our work using DFT revealed S_{max} to be indeed close to a mean-field spinodal for all the compounds studied. A detailed discussion on the true nature of S_{max} is beyond the scope of this work, and this aspect will be addressed in a future publication.

4.8. Induction Supersaturation ψ as Mean Metastable Zone Width $\langle S_n \rangle_0$. For the probability density given by eq 10, the mean energy barrier g_{mean} at which nucleation occurs in the limit of $r \rightarrow 0$ may be obtained as

$$g_{mean} = \int_0^\infty g f(g)\, dg = \int_0^\infty g \exp(-g)\, dg = 1 \qquad (16)$$

Hence, the mean supersaturation ψ at which one expects the first nucleus to form in an MZW experiment occurs at the condition $g_{mean} = 1$, i.e., at the supersaturation at which the energy barrier ΔG^* drops to 1 k_BT. From eq 11, one notes that the cumulative probability $F(g_{mean})$ at this mean energy barrier reaches a value of $(1/e) = 0.368$.

Typically, the characteristic time of nucleation for a system evolving at a constant supersaturation is obtained through induction time experiments in which one models the distribution of t_n using the CDF given by eq 8. The mean time τ, which represents the mean wait time for the first crystal at the supersaturation of experiment, is given by $\tau = (1/\kappa) = (1/JV)$ with $F(\tau) = (1 - 1/e)$.[20] This time τ represents the "induction time" of nucleation at a given supersaturation. In the same spirit, for the case of the metastable zone experiment, we define the mean supersaturation ψ at which the energy barrier drops to 1 k_BT as an *induction supersaturation*. At $S_n = \psi$ the cumulative probability of nucleation reaches $(1/e)$. The values of the induction supersaturation obtained for all of the compounds studied are provided in Table 3 and are shown in Figure 5.

Originating from eq 11, conceptually ψ represents a *path-independent* supersaturation at which one expects nucleation to occur on average in a system that is slowly supersaturated. This ψ is the same quantity as the path-independent "critical supersaturation" reported by He et al.[19] and is the same limiting supersaturation $\langle S_n \rangle_0$ from this work discussed in the context of Figure 1. We interpret this induction supersaturation ψ as an energetically determined lower limit to the metastable zone observed when a system is slowly and *continuously* supersaturated. Since the value of $F(g_{mean})$ at ψ (i.e., $P_{s=\psi}$) by definition is $(1/e)$ $(= 0.368)$, we note that for supersaturations below ψ, the probability of nucleation in a metastable zone experiment is small. This probability further decreases rapidly as one approaches the solubility point, i.e., as $S \rightarrow 1$ in eq 15.

Conceptually, at a given supersaturation (i.e., at a given p), the induction time τ characterizes the mean number of density fluctuations that need to occur before successful nucleation. By interpreting the rate of transition probability νp from eq 8 as the nucleation rate JV in the context of the CNT, one may obtain the nucleation rate parameters A and B through induction time experiments. The time of nucleation in a metastable zone experiment, however, does not characterize the "number of density fluctuations" that need to occur for successful nucleation. Effectively, t_n in this case characterizes only $p(g)$, and not ν (i.e., not J_0). Thus, no information can be obtained about the kinetic prefactor J_0 from the "time of nucleation" in an MZW experiment. The same implication applies to cooling crystallization experiments that focus on cooling rate as a determinant of the probability of nucleation. As a consequence, attempts to determine the kinetic factors of nucleation rate expression from a metastable zone experiment are error prone and need to be reevaluated.

4.9. Influence of Kinetics on the Metastable Zone Width. Thus far, we have discussed the probability of nucleation under the condition of continuously varying supersaturation in the limit of slow rate of change of supersaturation (the "low-r" regime). In this case, we have shown that nucleation occurs in a narrow range of supersaturations with a characteristic "induction" supersaturation ψ. Many studies reported in the literature, however, show consistently that higher rates of supersaturation lead to wider metastable zones. Indeed, our experiments also are in line with these reports. The results shown in Figure 1 indicate that as r is increased, the asymptotic nature of S_n disappears, and large values of S_n could be reached at higher rates of generation of supersaturation (e.g., at $r_n > 0.05$ h^{-1} for succinic acid and $r_n > 0.45$ h^{-1} for HEWL).

At a first glance, the notion that in a metastable zone the probability of nucleation is governed solely by the energetics of nucleation appears to go against this observed kinetic nature of the metastable zone width. To resolve this paradox, we need to focus on the nature of the density fluctuations that occur in the solution and on the concepts of equilibrium and steady-state. This aspect is discussed in detail in the Supporting Information. Here we limit the discussion by emphasizing that the "kinetic" effects involved in *our determination* of the limit of metastable zone manifest due to the process of equilibration of the system to a change in the supersaturation.

The characteristic time scale with which a system relaxes to a newly imposed change in the solution conditions is given by the time lag of nucleation (t_{lag}). The kinetic processes involved in the evolution of the system toward a steady-state may not be the same as the processes that govern nucleation at an already-achieved steady-state (i.e., processes that control the steady-state nucleation rate). We emphasize that the observed path dependence of an experimentally determined metastable zone width should *not* be attributed to a steady-state nucleation rate at each point along the path. This path dependence arises due to t_{lag}. This concept will be addressed in a future publication in which we shall show that the apparent shift in S_n as a function of r can be predicted accounting for the relaxation time t_{lag}, but without needing to consider a rate of nucleation.

DOI: 10.1021/acs.cgd.6b01529
Cryst. Growth Des. 2017, 17, 1132−1145

4.10. Effect of Solution Volume on the Metastable Zone Width. One of the key variables that is believed to influence the MZW is the volume of the system.[23−25] This expectation stems from the description of the MZW using the rate of nucleation J through eqs 3 and 4, which consider the product $J(t)V(t)$ as the rate of transition probability $\kappa(t)$. Thus, intuitively one would expect that the probability of nucleation should scale with the volume of the solution. Note that the Poisson description of nucleation that underlies the development of eq 8 does not consider the size of the system explicitly. This formulation considers only the number of attempts that occur *one after another* with a hypothetical attempt frequency of ν.

One might expect the attempt frequency ν to scale with solution volume V. And so, it is reasonable to expect $F(t)$ to scale with V, but only when the system evolves at a constant supersaturation, i.e., in an induction time experiment. In a metastable zone experiment, as opposed to an induction time experiment, the probability of nucleation does not depend on ν. The variable p, which determines the nucleation probability in this scenario, itself cannot have volume dependence because p is interpreted in the time average sense, and not in the ensemble average sense (see Supporting Information). As a result, a consistent Poisson model for nucleation under time-varying supersaturation does not predict the probability of nucleation to depend on the volume of the solution, provided that the experiment is conducted in the limit of $r \to 0$. More discussion on other possible volume effects on the observed MZW is provided in the Supporting Information.

5. CONCLUSIONS

The stochastic nature of nucleation originates from the randomness involved in the appearance of the "clusters" of foreign phase in a medium through spontaneous density fluctuations. Historically, the Markov (Poisson) description of nucleation was conceived to extract useful "kinetic" information on nucleation from experiments at constant supersaturation. Thus, in essence, an experimental probability distribution $F(t)$ at a given supersaturation "defines" the *stochastic* (average) nucleation rate at that supersaturation and not *vice versa*.[48] This distinction between the probabilistic (Markov) and mechanistic (CNT) views of nucleation was not emphasized in later publications. The notion that nucleation rate (usually from CNT) is *the cause* of the stochasticity of nucleation is widely implied in modern literature, whereas it is only *a hypothesis* needed to facilitate a time-continuous Poisson description of a discrete process. The Poisson model, originally conceived to be applicable to nucleation at constant supersaturation, has been extended later to describe nucleation under time-varying supersaturation. This extension, which considers a time-dependent nucleation rate as the "driver" for the nucleation probability, is not consistent with the physics of the underlying Poisson process. The resulting theoretical approximation may lead to incorrect predictions and conclusions, as seen from our experimental data in Figure 4a−d.

The concept discussed in this work is simple: a differential limit of $dt \to 0$ is only a mathematical convenience that facilitates a time-continuous description of the nucleation process at a constant supersaturation. This limit cannot be interpreted as $dt = 0$ since time has to evolve. When the supersaturation of a system is *continuously* varied, the system cannot "wait" for any nonzero time interval dt at any S. Representing the transition probability during that dt as $\kappa(t)\,dt$ is thus questionable and is not in line with the underlying physical description of the process. Hence, strictly speaking, the notion of a nucleation rate is not relevant for the analysis of an MZW experiment. While this differential *approximation* is widely used in the literature to various degrees of success, our work for the first time presents experimental data that highlights the limitation of this approach.

A prevalent notion that stems from the existing approach is that, in an MZW experiment, in the limiting case $r \to 0$, the system must nucleate close to the solubility boundary.[21] One can even find in the literature methods of solubility determination based on this notion! We note that the limit $r \to 0$ cannot be interpreted as $r = 0$, because S has to change for the progress of an MZW experiment. Within the scope of the Poisson description that gives meaning to the stochastic approach, when S is continuously varied, the solubility boundary *at most* experiences one density fluctuation. The probability for that fluctuation to be a critical fluctuation is zero. Thus, we conclude that, in a metastable zone experiment, as $r \to 0$, the system does not nucleate at the solubility boundary. Instead, in this limit, the probability of nucleation at any supersaturation is dictated by eqs 10 and 11.

The reasons discussed above suggest that attempts to obtain nucleation rate parameters from the MZW experiments can be misleading. Any agreement observed between the "rate models" (e.g., eq 1) and the experimental data in terms of the time (or the temperature, in the case of cooling crystallization) of nucleation may be fortuitous. One needs to assess the validity of these models on the basis of the supersaturation of nucleation to uncover any hidden disagreements. This need was demonstrated in this work through Figures 3a−d and 4a−d. For the same reasons, comparing experimental data on MZW in cooling crystallization on the basis of the rate of cooling is not recommended. Instead, it is more appropriate to translate the experimental results and compare them on the basis of the rate of generation of driving force.

When a system is slowly and continuously supersaturated, one expects the system to nucleate at a mean "induction supersaturation" that corresponds to an energy barrier of 1 k_BT. On a first glance, the concept of an induction supersaturation introduced through eq 15 may appear as an obvious conclusion. After all, one intuitively expects that during a gradual decrease of energy barrier, when the energy barrier drops to the levels of thermal energy, nucleation should occur effortlessly. Indeed, such intuitiveness is *the* appealing aspect of eq 15, which is missing from the existing approaches that focus on time of nucleation through eq 1. Depending on the volume of the system considered, eq 1 may not predict a short mean time of nucleation even when the energy barrier drops to thermal energy levels.

The Poisson model of nucleation as a rare success obtained through many attempts is rather rudimentary and is an approximation. Current understanding of nucleation pathways under gradually increasing supersaturation is limited. The fundamental modes of phase separation—nucleation and spinodal decomposition—are of intense focus in many investigations over the past several decades[42,54,55,62−65] Indeed, "kinetic spinodals" that occur at energy barriers of a few k_BT were proposed in the literature as "observable limits of metastability".[64] Such fundamental aspects of nucleation pathways (e.g., a two-step nucleation pathway) are beyond the scope of the approximate Poisson models such as eq 4 or eq 11. However, eq 11 has an intuitive appeal in this regard that is not present in eq 4. Further, a mean induction supersaturation of nucleation (ψ) at $\Delta G^* = 1\ k_BT$ is within the realm of the kinetic spinodals discussed in these studies of phase separation.

DOI: 10.1021/acs.cgd.6b01529
Cryst. Growth Des. 2017, 17, 1132−1145

The stochastic models discussed in this work are not concerned with exactly how a system produces the density fluctuations "one after another", a necessary condition for a Poisson process. This detail of the "nucleation mechanism" comes into focus only when one attempts to express the probability of success p in terms of the energy barrier (through eq 12) or the rate of transition probability κ in terms of the nucleation rate (through eq 2). Although we have used the CNT ("one-step" nucleation) description for the energy barrier in this work, the experimental data could be explained equally well by considering a nucleus to be a "dense liquid droplet" (two-step nucleation) and using DFT arguments to obtain the energy barrier. This aspect will be discussed in a future publication.

The concept of an induction supersaturation as an energetically driven lower limit of metastability is of practical relevance. This ψ can be interpreted as a "*lower*" limit of metastable zone that can be estimated quickly for many systems through eq 15 with $P_s = (1/e)$. The interfacial free energy (Γ) needed for this calculation may be estimated from the knowledge of the solubility of a compound.[59] This lower limit provides a guideline for a wide range of applications that involve growing crystals under conditions of low supersaturation.

In this work, we mainly discussed the probability of nucleation in an MZW experiment in the low-r regime. Our future work will focus on the true nature of S_{max} and on the prediction of this probability in the high-r regime accounting for the lag-time effects. We hope that the general observations presented in this work for a variety of compounds open doors to a different way of thinking regarding the origins of the metastable zone and the mechanisms of solid−liquid phase separation.

■ ASSOCIATED CONTENT

Supporting Information

The Supporting Information is available free of charge on the ACS Publications website at DOI: 10.1021/acs.cgd.6b01529.

Available Supporting Information includes (i) a mass balance model that describes the time dependence of supersaturation S and of rate of change of driving force r, (ii) extended discussion on the stochastic analysis of nucleation, derivation of the Master equation, and the probabilistic relevance of the nucleation rate, (iii) extended discussion on the path dependence of the metastable zone width, and (iv) extended discussion on the effect of solution volume on the metastable zone width (PDF)

■ AUTHOR INFORMATION

Corresponding Author

*E-mail: vbhamidi@eastman.com.

ORCID

Venkateswarlu Bhamidi: 0000-0003-1875-0574

Paul J. A. Kenis: 0000-0001-7348-0381

Present Address

†(V.B.) Scale-up and Process Innovation, Eastman Chemical Company, Kingsport, TN 37662−5167, USA.

Notes

The authors declare no competing financial interest.

■ ACKNOWLEDGMENTS

We acknowledge Prof. R. D. Braatz (Massachusetts Institute of Technology), Prof. Baron Peters (University of California, Santa Barbara), Dr. Ryan Larsen (University of Illinois at Urbana−Champaign), Dr. Sameer Talreja (BP, Naperville, USA), and Dr. Guangwen He (Procter & Gamble, Singapore) for stimulating discussions. V.B. thanks Dr. Meenesh Singh (University of Illinois at Chicago) and Dr. Debangshu Guha (Eastman Chemical Company) for inspiring conversations. High quality graphics from Microsoft Excel plots were generated using Daniel's XL Toolbox add-in for Excel (v 6.6), a free utility created by Daniel Kraus, Würzburg, Germany. We gratefully acknowledge financial support from University of Illinois and Institute of Chemical and Engineering Sciences (ICES), Singapore.

■ REFERENCES

(1) Thanh, N. K. T.; Maclean, N. M.; Mahiddine, S. Mechanisms of Nucleation and Growth of Nanoparticles in Solution. *Chem. Rev.* **2014**, *114*, 7610−7630.

(2) Chayen, N. E. Turning Protein Crystallisation from an Art into a Science. *Curr. Opin. Struct. Biol.* **2004**, *14*, 577−583.

(3) Blundell, T. L.; Jhoti, H.; Abell, C. High-throughput Crystallography for Lead Discovery in Drug Design. *Nat. Rev. Drug Discovery* **2002**, *1*, 45−54.

(4) Pande, A.; Pande, J.; Asherie, N.; Lomakin, A.; Ogun, O.; King, J.; Benedek, G. B. Crystal Cataracts: Human Genetic Cataract Caused by Protein Crystallization. *Proc. Natl. Acad. Sci. U. S. A.* **2001**, *98*, 6116−6120.

(5) Rodríguez-Hornedo, N.; Murphy, D. Significance of Controlling Crystallization Mechanisms and Kinetics in Pharmaceutical Systems. *J. Pharm. Sci.* **1999**, *88*, 651−660.

(6) Cerini, C.; Geider, S.; Dussol, B.; Hennequin, C.; Daudon, M.; Veesler, S.; Nitsche, S.; Boistelle, R.; Berthézène, P.; Dupuy, P.; Vazi, A.; Berland, Y.; Dagorn, J.-C.; Verdier, J.-M. Nucleation of Calcium Oxalate Crystals by Albumin: Involvement in the Prevention of Stone formation. *Kidney Int.* **1999**, *55*, 1776−1786.

(7) Schwartz, A. M.; Myerson, A. S. Solutions and Solution Properties. In *Handbook of Industrial Crystallization*, 2nd ed.; Myerson, A. S., Ed.; Butterworth-Heinemann: Woburn, 2002.

(8) Fujiwara, M.; Chow, P. S.; Ma, D. L.; Braatz, R. D. Paracetamol Crystallization Using Laser Backscattering and ATR-FTIR Spectroscopy: Metastability, Agglomeration, and Control. *Cryst. Growth Des.* **2002**, *2*, 363−370.

(9) More correctly, supersaturation is defined as the ratio of activity of the solute at a given condition to the activity of the solute at equilibrium. For dilute solutions, the activity coefficients, and/or their ratio, often approach unity, and supersaturation is typically expressed as C/C_{eq} with sufficient accuracy.

(10) Bonnin-Paris, J.; Bostyn, S.; Havet, J.-L.; Fauduet, H. Determination of the Metastable Zone Width of Glycine Aqueous Solutions for Batch Crystallizations. *Chem. Eng. Commun.* **2011**, *198*, 1004−1017.

(11) Sahin, O.; Dolas, H.; Demir, H. Determination of Nucleation Kinetics of Potassium Tetraborate Tetrahydrate. *Cryst. Res. Technol.* **2007**, *42*, 766−772.

(12) Kashchiev, D.; Borissova, A.; Hammond, R. B.; Roberts, K. J. Effect of Cooling Rate on the Critical Undercooling for Crystallization. *J. Cryst. Growth* **2010**, *312*, 698−704.

(13) Sangwal, K. A Novel Self-Consistent Nývlt-like Equation for Metastable Zone Width Determined by the Polythermal Method. *Cryst. Res. Technol.* **2009**, *44*, 231−247.

(14) Sangwal, K. Novel Approach to Analyze Metastable Zone Width Determined by the Polythermal Method: Physical Interpretation of Various Parameters. *Cryst. Growth Des.* **2009**, *9*, 942−950.

(15) Kim, K.-J.; Mersmann, A. Estimation of Metastable Zone Width in Different Nucleation Processes. *Chem. Eng. Sci.* **2001**, *56*, 2315−2324.

(16) Mersmann, A.; Bartosch, K. How to Predict the Metastable Zone Width. *J. Cryst. Growth* **1998**, *183*, 240−250.

(17) Nývlt, J. Kinetics of Nucleation in Solutions. *J. Cryst. Growth* **1968**, *3*−*4*, 377−383.

DOI: 10.1021/acs.cgd.6b01529
Cryst. Growth Des. 2017, 17, 1132−1145

(18) Sear, R. P. Quantitative Studies of Crystal Nucleation at Constant Supersaturation: Experimental Data and Models. *CrystEngComm* **2014**, *16*, 6506−6522.
(19) He, G.; Bhamidi, V.; Tan, R. B. H.; Kenis, P. J. A.; Zukoski, C. F. Determination of Critical Supersaturation from Microdroplet Evaporation Experiments. *Cryst. Growth Des.* **2006**, *6*, 1175−1180.
(20) Goh, L.; Chen, K.; Bhamidi, V.; He, G.; Kee, N. C. S.; Kenis, P. J. A.; Zukoski, C. F.; Braatz, R. D. A Stochastic Model for Nucleation Kinetics Determination in Droplet-Based Microfluidic Systems. *Cryst. Growth Des.* **2010**, *10*, 2515−2521.
(21) Peters, B. Supersaturation Rates and Schedules: Nucleation Kinetics from Isothermal Metastable Zone Widths. *J. Cryst. Growth* **2011**, *317*, 79−83.
(22) Kashchiev, D.; Firoozabadi, A. Kinetics of the Initial Stage of Isothermal Gas Phase Formation. *J. Chem. Phys.* **1993**, *98*, 4690−4699.
(23) Kadam, S. S.; Kramer, H. J. M.; ter Horst, J. H. Combination of a Single Primary Nucleation Event and Secondary Nucleation in Crystallization Processes. *Cryst. Growth Des.* **2011**, *11*, 1271−1277.
(24) Kadam, S. S.; Kulkarni, S. A.; Ribera, R. C.; Stankiewicz, A. I.; ter Horst, J. H.; Kramer, H. J. M. A New View on the Metastable Zone Width During Cooling Crystallization. *Chem. Eng. Sci.* **2012**, *72*, 10−19.
(25) Maggioni, G. M.; Mazzotti, M. Modelling the Stochastic Behaviour of Primary Nucleation. *Faraday Discuss.* **2015**, *179*, 359−382.
(26) Sangwal, K. Recent Developments in Understanding of the Metastable Zone Width of Different Solute-Solvent Systems. *J. Cryst. Growth* **2011**, *318*, 103−109.
(27) Talreja, S.; Perry, S. L.; Guha, S.; Bhamidi, V.; Zukoski, C. F.; Kenis, P. J. A. Determination of the Phase Diagram for Soluble and Membrane Proteins. *J. Phys. Chem. B* **2010**, *114*, 4432−4441.
(28) He, G.; Bhamidi, V.; Wilson, S. R.; Tan, R. B. H.; Kenis, P. J. A.; Zukoski, C. F. Direct Growth of γ-Glycine from Neutral Aqueous Solutions by Slow, Evaporation-Driven Crystallization. *Cryst. Growth Des.* **2006**, *6*, 1746−1749.
(29) Davies, M.; Griffiths, D. M. L. The Solubilities of Dicarboxylic Acids in Benzene and Aqueous Solutions. *Trans. Faraday Soc.* **1953**, *49*, 1405−1410.
(30) Kustov, A. V.; Korolev, V. P. The Thermodynamic Characteristics of Solution of L-α-Histidine and L-α-Phenylalanine in Water at 273−373 K. *Phys. Chem. of Solns.* **2008**, *82*, 1828−1832.
(31) Granberg, R. A.; Rasmuson, Å. C. Solubility of Paracetamol in Pure Solvents. *J. Chem. Eng. Data* **1999**, *44*, 1391−1395.
(32) Forsythe, E. L.; Pusey, M. L. The Effects of Acetate Buffer Concentration on Lysozyme Solubility. *J. Cryst. Growth* **1996**, *168*, 112−117.
(33) Finnie, S. D.; Ristic, R. I.; Sherwood, J. N.; Zikic, A. M. Morphological and Growth Rate Distributions of Small Self-nucleated Paracetamol Crystals Grown from Pure Aqueous Solutions. *J. Cryst. Growth* **1999**, *207*, 308−318.
(34) Mullin, J. W.; Whiting, J. L. Succinic Acid Crystal Growth Rates in Aqueous Solution. *Ind. Eng. Chem. Fundam.* **1980**, *19*, 117−121.
(35) Forsythe, E. L.; Pusey, M. L. The Effects of Temperature and NaCl Concentration on Tetragonal Lysozyme Face Growth Rates. *J. Cryst. Growth* **1994**, *139*, 89−94.
(36) The definition of the "average supersaturation" $\langle S_n \rangle$ is clarified in Section 4.8.
(37) Kashchiev, D.; van Rosmalen, G. M. Review: Nucleation in Solutions Revisited. *Cryst. Res. Technol.* **2003**, *38*, 555−574.
(38) Kashchiev, D.; Verdoes, D.; van Rosmalen, G. M. Induction Time and Metastability Limit in New Phase Formation. *J. Cryst. Growth* **1991**, *110*, 373−380.
(39) Typically, when employing these models, one assumes that lag time effects in nucleation are unimportant, and considers the system to be "equilibrated" to the prevailing supersaturation at any time.
(40) Kashchiev, D. *Nucleation: Basic Theory with Applications*, 1st ed.; Butterworth-Heinemann: Boston, USA, 2000; p 529.
(41) Chen, K.; Goh, L.; He, G.; Kenis, P. J. A.; Zukoski, C. F.; Braatz, R. D. Identification of Nucleation Rates in Droplet-based Microfluidic Systems. *Chem. Eng. Sci.* **2012**, *77*, 235−241.
(42) Vekilov, P. G. Two-step Mechanism for the Nucleation of Crystals from Solution. *J. Cryst. Growth* **2005**, *275*, 65−76.
(43) Van Kampen, N. G. *Stochastic Processes in Physics and Chemistry*, 3rd ed.; Elsevier: Amsterdam, The Netherlands, 2007; p 464.
(44) Gardiner, C. W. *Handbook of Stochastic Methods*, 2nd ed.; Springer-Verlag: Berlin, Germany, 1985.
(45) Strictly speaking, the phrase "the probability of nucleation" is somewhat ambiguous, because a cluster size that differentiates a nucleus from a fully grown "crystal" is not very well defined. While we recognize that a critical cluster need not necessarily grow into a crystal, in line with the conventional interpretation, here we consider the term "nucleus" to mean the "critical cluster". This is the same meaning behind the exponential term in eq 2.
(46) Ford, I. J. Statistical Mechanics of Nucleation: A Review. *Proc. Instn Mech. Eng.* **2004**, *218* (PartC), 883−899.
(47) ten Wolde, P. R.; Frenkel, D. Enhancement of Protein Crystal Nucleation by Critical Density Fluctuations. *Science* **1997**, *277*, 1975−1977.
(48) Toschev, S.; Milchev, A.; Stoyanov, S. On Some Probabilistic Aspects of the Nucleation Process. *J. Cryst. Growth* **1972**, *13-14*, 123−127.
(49) The other part of the uncertainty is whether an attempt by the system will be successful in crossing the prevailing energy barrier. Note that a measure of this uncertainty is given by *p* and not by the nucleation rate *J*.
(50) Debenedetti, P. G. *Metastable Liquids: Concepts and Principles*, 1st ed.; Princeton University Press: Princeton, USA, 1996.
(51) Oxtoby, D. W. Nucleation of First-Order Phase Transitions. *Acc. Chem. Res.* **1998**, *31*, 91−97.
(52) Oxtoby, D. W.; Evans, R. Nonclassical Nucleation Theory for the Gas-Liquid Transition. *J. Chem. Phys.* **1988**, *89*, 7521−7530.
(53) Auer, S.; Frenkel, D. Prediction of Absolute Crystal Nucleation Rate in Hard-Sphere Colloids. *Nature* **2001**, *409*, 1020−1023.
(54) Binder, K. Nucleation Barriers, Spinodals, and the Ginzburg Criterion. *Phys. Rev. A: At., Mol., Opt. Phys.* **1984**, *29*, 341−349.
(55) Cahn, J. W.; Hilliard, J. E. Free Energy of a Nonuniform System. III. Nucleation in a Two-Component Incompressible Fluid. *J. Chem. Phys.* **1959**, *31*, 688−699.
(56) Granberg, R. A.; Ducreux, C.; Gracin, S.; Rasmuson, Å. C. Primary Nucleation of Paracetamol in Acetone−Water Mixtures. *Chem. Eng. Sci.* **2001**, *56*, 2305−2313.
(57) Kulkarni, A. M.; Zukoski, C. F. Nanoparticle Crystal Nucleation: Influence of Solution Conditions. *Langmuir* **2002**, *18*, 3090−3099.
(58) Sear, R. P. Classical Nucleation Theory for the Nucleation of the Solid Phase of Spherical Particles with a Short-ranged Attraction. *J. Chem. Phys.* **1999**, *111*, 2001−2007.
(59) Christoffersen, J.; Rostrup, E.; Christoffersen, M. R. Relation Between Interfacial Surface Tension of Electrolyte Crystals in Aqueous Suspension and Their Solubility; A Simple Derivation Based on Surface Nucleation. *J. Cryst. Growth* **1991**, *113*, 599−605.
(60) Kashchiev, D. Thermodynamically Consistent Description of the Work to Form a Nucleus of any Size. *J. Chem. Phys.* **2003**, *118*, 1837−1851.
(61) Wilemski, G. The Kelvin Equation and Self-Consistent Nucleation Theory. *J. Chem. Phys.* **1995**, *103*, 1119−1126.
(62) Shah, M.; Galkin, O.; Vekilov, P. G. Smooth Transition from Metastability to Instability in Phase Separating Protein Solutions. *J. Chem. Phys.* **2004**, *121*, 7505−7512.
(63) Balsara, N. P.; Rappl, T. J.; Lefebvre, A. A. Does Conventional Nucleation Occur during Phase Separation in Polymer Blends? *J. Polym. Sci., Part B: Polym. Phys.* **2004**, *42*, 1793−1809.
(64) Wang, Z.-G. Concentration Fluctuation in Binary Polymer Blends: χ Parameter, Spinodal and Ginzburg Criterion. *J. Chem. Phys.* **2002**, *117*, 481−500.
(65) Cahn, J. W.; Hilliard, J. E. Free Energy of a Nonuniform System. I. Interfacial Free Energy. *J. Chem. Phys.* **1958**, *28*, 258−267.

DOI: 10.1021/acs.cgd.6b01529
Cryst. Growth Des. 2017, 17, 1132−1145